Insulin Receptor Autophosphorylation. I. Autophosphorylation Kinetics of the Native Receptor and Its Cytoplasmic Kinase Domain†

R. A. Kohanski

Department of Biochemistry, The Mount Sinai School of Medicine, 1 Gustave L. Levy Place, New York, New York 10029

Received October 6, 1992; Revised Manuscript Received March 12, 1993

ABSTRACT: Kinetic analysis of autophosphorylation was done using a non-Michaelis–Menten kinetic model. This model describes autophosphorylation in terms of a fast reaction phase, a slow reaction phase, and a partition function for the two phases. Kinetic parameters determined by this new approach show that insulin stimulates autophosphorylation by promoting (1) a 10-fold increase in the rate constant for the fast phase of the reaction and (2) a 2-fold increase in the partition function favoring the fast phase. Insulin did not significantly affect the binding constant for ATP in this fast phase. Kinetic parameters obtained for the cytoplasmic kinase domain were similar to those obtained for the native insulin receptor *in the absence of insulin.* The insulin receptor has three subdomains encompassing its seven autophosphorylation sites. The juxtamembrane sites react primarily in the slow kinetic phase, favored by the absence of stimulation and low ATP concentrations. The carboxy-terminal and central autophosphorylation subdomains react primarily in the fast kinetic phase, favored by raising the ATP concentration and/or the presence of insulin. These observations demonstrate that (1) both ATP and insulin regulate reaction in each autophosphorylation subdomain, (2) insulin stimulation occurs predominantly in the central and carboxy-terminal regions, and (3) autophosphorylation observed with the cytoplasmic kinase domain was similar to native insulin receptor *in the absence of insulin.* These findings are consistent with conclusions based on the kinetic analysis of autophosphorylation.

The native insulin receptor/protein(tyrosine) kinase contains two insulin binding α-subunits and two β-subunits that cross the plasma membrane and bear the protein kinase domain. Insulin stimulates autophosphorylation of the receptor within this intracellular domain, and this leads to activation of substrate phosphorylation [cf. reviews by Ellis *et al.* (1991) and Olefsky, (1990)]. There are three subdomains that undergo autophosphorylation, including seven discrete tyrosine residues of the β-subunit (Ellis et al., 1986; Flores Riveros et al., 1989; Herrera & Rosen, 1986; Murakami & Rosen, 1991; Tornqvist & Avruch, 1988; White et al., 1988), two of which are first identified in the following paper in this issue (Kohanski, 1993). The isolated cytoplasmic kinase domain of the insulin receptor has been expressed using insect cell cultures and the baculovirus expression system (Cobb *et al.*, 1989; Villalba *et al.*, 1989). Both groups have shown that autophosphorylation of this form of the enzyme also leads to activation of substrate phosphorylation.

Autophosphorylation is a bench mark reaction of most protein kinases, with consequences for the regulation of their enzyme activities. For example, autophosphorylation of the Ca^{2+}/calmodulin-dependent protein kinase II alters its dependence upon these activators (Lai *et al.*, 1986). Autophosphorylation of the Ca^{2+}-activated phospholipid-dependent protein kinase from rat brain results in a lowered K_a for Ca^{2+} activation (Huang *et al.*, 1986). The cyclic-AMP-dependent protein kinase undergoes autophosphorylation that affects the reassociation of the regulatory and catalytic subunits (Rosen & Erlichman, 1975). Phosphorylase kinase undergoes autophosphorylation which is subject to multiple levels of regulation (Wang *et al.*, 1976; Carlson & Graves, 1976; Hallenbeck & Walsh, 1983). In these and numerous other examples including the growth factor receptor protein kinases (cf. Ullrich & Schlessinger, 1990; Riedel *et al.*, 1989), autophosphorylation is under strict regulation by specific effectors of the enzyme.

Despite the prevalence of this reaction and its importance in biological regulation, the mechanisms by which autophosphorylation are stimulated are poorly understood. To further this understanding, we have undertaken a novel kinetic analysis of insulin receptor autophosphorylation. The analysis shows the basis for insulin stimulation of autophosphorylation, that the isolated cytoplasmic kinase domain autophosphorylates as an unstimulated enzyme, and together with the following paper gives additional details on stimulatory effect of insulin within each subdomain of the native receptor that undergo autophosphorylation.

EXPERIMENTAL PROCEDURES

Materials. [^{32}P]Orthophosphate was obtained from ICN Radiochemicals. [γ-^{32}P]ATP was synthesized according to published procedures (Walseth & Johnson, 1979) and purified (Palmer & Avruch, 1981). HEPES,[1] DTT, ATP, and electrophoresis reagents were from Boehringer/Mannheim Biochemicals. Trypsin was from Boehringer/Mannheim. Matrices and high-pressure columns are described in the following paper (Kohanski, 1993). The intact 48-kDa cytoplasmic kinase domain (CKD) of the human insulin receptor was expressed in Sf9 cells and purified, essentially as described (Villalba et al., 1989). Cell culture reagents were from Gibco. The recombinant baculovirus containing cDNA for the CKD was a gift of the late Dr. Ora Rosen. The NIH 3T3 cell line overexpressing the human insulin receptor was the gift of Dr. J. Whittaker (Whittaker et al., 1987). Insulin receptor from

† Supported by Grant DK 38893 from the National Institutes of Health.

[1] Abbreviations: CKD, cytoplasmic kinase domain of the human insulin receptor; DTT, dithiothreitol; HEPES, 4-(2-hydroxyethyl-1-piperazine)ethanesulfonic acid; HPLC, high-performance liquid chromatography; SDS–PAGE, sodium dodecyl sulfate–polyacrylamide gel electrophoresis; Tris, tris(hydroxymethyl)aminomethane.

0006-2960/93/0432-5766$04.00/0

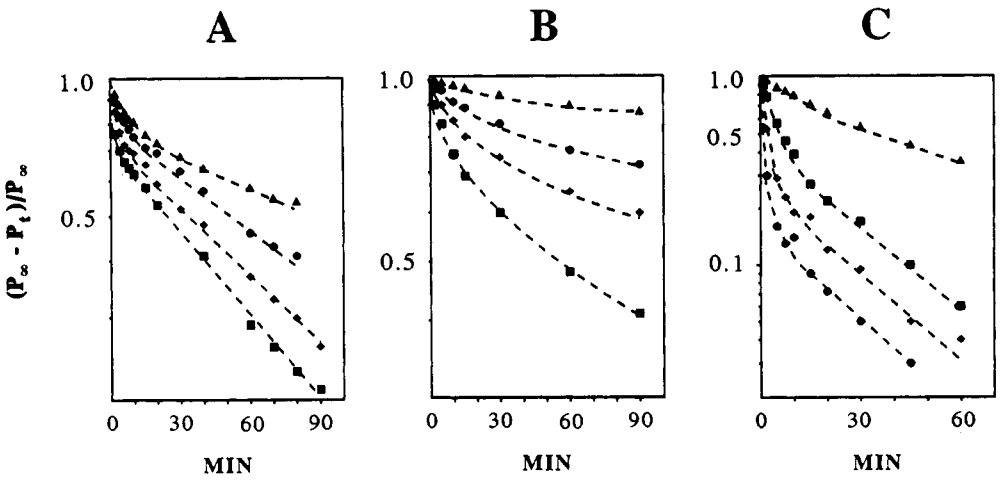

FIGURE 1: Semilogarithmic plots of the time courses of autophosphorylation. (Panel A) Autophosphorylation of the purified cytoplasmic kinase domain at the following concentrations of [γ-^{32}P]ATP: 50 μM (△); 100 μM (○); 200 μM (◆); 400 μM (■). Data are shown in terms of the fraction of enzyme remaining to be autophosphorylated = $(P_\infty - P_t)/(P_\infty)$, as described by eq 5 under Results. (Panel B) The purified native insulin receptor in the absence of insulin. (Panel C) The purified native insulin receptor at 1 μM insulin. For panels B and C, the concentrations of [γ-^{32}P]ATP were 5 μM (△); 20 μM (○); 50 μM (◆); 100 μM (■).

these cells was purified as described previously (Kohanski & Schenker, 1991). ^{125}I-labeled insulin was prepared, and binding to solubilized receptor was done as described (Kohanski & Lane, 1983).

Time Courses of Autophosphorylation. The reactions with purified insulin receptor were done in the absence or presence of 1 μM insulin. The buffer was 50 mM HEPES, pH 7.0. $Mn(CH_3CO_2)_2$ was present at a final concentration of 5 mM. The receptor was present at a concentration of 2.2 nM, based upon insulin binding sites, and [γ-^{32}P]ATP was used over the concentration range 5–100 μM at a single specific activity of ≈73 600 cpm/pmol (≈0.12 μCi/pmol, measured at the time of data collection by Cherenkov counting). Aliquots of 50 μL each were taken from the reaction mixture at timed intervals between 1 and 90 min and quenched by the addition of concentrated electrophoresis sample buffer, and the ^{32}P-labeled β-subunit was isolated by SDS–PAGE using the system of Laemmli (1970). The reactions with purified CKD were done at 0.5 μM enzyme, based upon its molar absorptivity at 280 nm (Villalba et al., 1989), and [γ-^{32}P]ATP was used over the concentration range 50–400 μM at a single specific activity of 33 150 cpm/pmol (≈0.05 μCi/pmol). Bovine serum albumin was present at 0.01% (w/v). The buffer was 50 mM HEPES, pH 7.0, containing DTT at 0.5 mM final concentration. Aliquots of 40 μL each were taken at timed intervals between 1 and 80 min and quenched, and the ^{32}P-labeled CKD was isolated as described above. For all sets of reactions, aliquots were also taken after 5 h and 6–8 h to determine the endpoint of the reactions. All reactions were done at room temperature. Data analysis was done using the equations given under Results. Both graphical methods and nonlinear regression for data fitting were done.

Autophosphorylation for Tryptic [^{32}P]Phosphopeptide Mapping. Thirty-minute autophosphorylation reactions were performed with native insulin receptor in the absence or presence of 1 μM insulin. The concentration of receptor was approximately that used for the kinetic experiments. The concentration of CKD was 0.15 μM. These reactions were quenched by the addition of ice-cold trichloroacetic acid to a final concentration of 20%, using 10 μg of bovine serum albumin as carrier. The concentrations of [γ-^{32}P]ATP used are given under Results, and various specific activities were used for these reactions, although a single specific activity was used at each concentration of [γ-^{32}P]ATP to compare the basal and insulin-stimulated reactions with the native receptor. To generate tryptic [^{32}P]phosphopeptide maps by reverse-phase HPLC, the ^{32}P-labeled enzymes were isolated by SDS–PAGE and trypsinized from wet gel segments. The resulting [^{32}P]phosphopeptide were resolved by reverse-phase HPLC, using on-line detection of ^{32}P by a Radiomatic Flo-One Beta continuous flow detector. Exact details for these protocols are given in the following paper (Kohanski, 1993), wherein the identities of each mapped [^{32}P]phosphopeptide are established.

RESULTS

Kinetics of Autophosphorylation. We examined extended time courses of autophosphorylation at different concentrations of [γ-^{32}P]ATP. The reaction endpoints determined as described under Experimental Procedures were invariant within a range of ±5% yielding a stoichiometry of 3.5 pmol of ^{32}P/pmol of kinase. This was found for the CKD and the native insulin receptor in the absence or presence of insulin, determined by mass or per insulin binding site, respectively. The semilogarithmic replot of data from the time courses were biphasic, indicating that the reaction could be described by the sum of two exponentials (Figure 1). The extent of autophosphorylation at any time during the reaction, described in terms of the reaction's endpoint, is given by

$$P_t = P_\infty(1 - \phi_f e^{-k_I^{obs}t} - \phi_s e^{-k_{II}^{obs}t}) \quad (1)$$

The amount of autophosphorylation at endpoint is given by P_∞, and is determined experimentally. Net autophosphorylation of the kinase after a given time of reaction, P_t, is the result of contributions from two reaction rates governed by k_I^{obs} for the fast phase and k_{II}^{obs} for the slow phase. How much each phase contributes to the net reaction is determined by three ATP-dependent parameters (eq 2 and 3, and eq 4, below):

$$k_I^{obs} = \frac{k_I[ATP]}{K_I + [ATP]} \quad (2)$$

$$k_{II}^{obs} = \frac{k_{II}[ATP]}{K_{II} + [ATP]} \quad (3)$$

While it is possible that either the fast or slow phases could

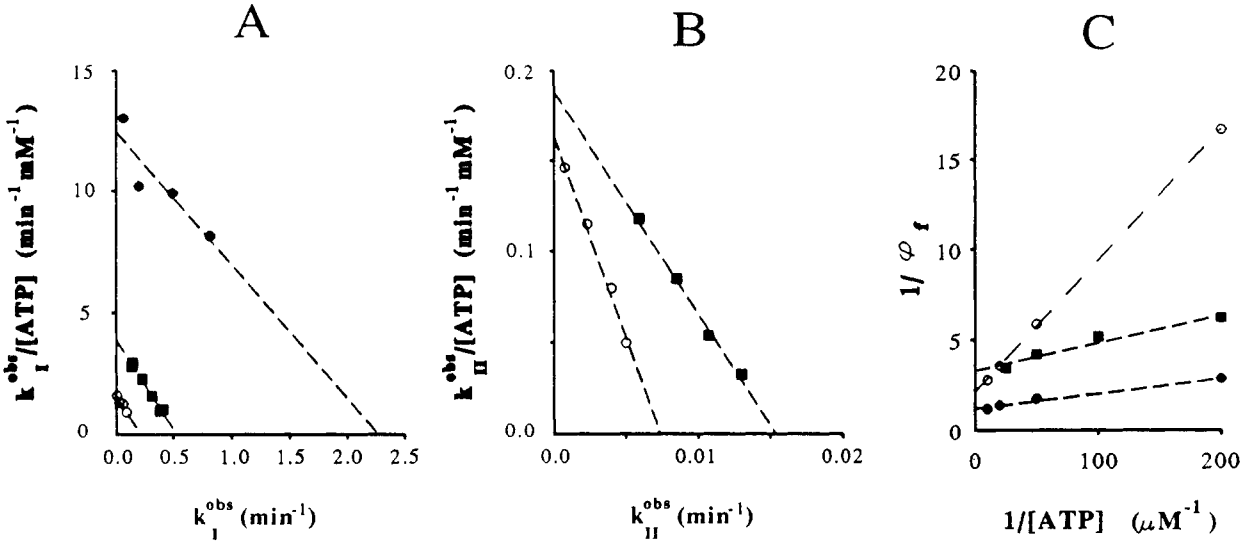

FIGURE 2: Saturation of the observed rate constants and the partition function with increasing ATP concentration. Rate constants for the fast phase (k_I^{obs}, panel A), for the slow phase (k_{II}^{obs}, panel B), and for the partition function ϕ_f (panel C) were replotted. Each X-axis intercept in the Eadie–Skatchard plots gives the intrinsic rate constant, and the negative reciprocal of each slope gives the ATP-dissociation constants for these phases. Panel C uses the format for a Lineweaver–Burk plot. Data for the CKD (■), the native insulin receptor in the absence (○) or presence of 1 μM insulin (●), were derived from Figure 1.

represent simple bimolecular reactions, the data described below support saturable functions for both reaction phases; i.e., the formation of a reversible complex between enzyme and metal-ATP that precedes the phosphoryl transfer step. The observed reaction rates for each phase, at fixed [ATP], are determined by k_I and k_{II}, the intrinsic rate constants for the fast and slow phases, respectively, and K_I and K_{II}, the dissociation constants for ATP binding leading to the fast and slow phases, respectively. The intrinsic rate constants are analogous to maximal velocities in that they represent the maximum rates at saturating ATP concentrations. In addition, there is a function that describes the fraction of the kinase that reacts by the slow phase versus the fast phase at the start of the reaction and at a given ATP concentration:

$$\phi_f = 1 - \phi_s = \frac{\Phi_f[ATP]}{K_f + [ATP]} \quad (4)$$

where Φ_f is the fraction of the reaction that proceeds initially by the fast phase at saturating ATP concentrations. The dissociation constant for ATP that determines this distribution is given by K_f.

In summary, the autophosphorylation reaction is described by saturable fast and slow reaction rates (the sum of two exponentials). The fractional division between these phases is also dependent upon the ATP concentration. With this model, it is possible to describe the stimulatory effect of insulin on the autophosphorylation reaction. It is also possible to compare the native insulin receptor with the cytoplasmic kinase domain.

These equations were used to analyze data from time courses of autophosphorylation, and the rate constants were also graphically extracted using a rearrangement of eq 1 to depict the data as the sum of two exponential decays:

$$\frac{P_\infty - P_t}{P_\infty} = \phi_f e^{-k_I^{obs} t} + \phi_s e^{-k_{II}^{obs} t} \quad (5)$$

For graphical analysis, plotting the data according to eq 5 was more convenient (Figure 1). The initial part of the reaction represents both phases, and the second part of the reaction is dominated by the slow phase. Thus the observed rate for the slow phase (k_{II}^{obs}) can be estimated by considering data after the fast reaction phase has "decayed". In addition, the fraction initially disposed to proceed by the slow phase (ϕ_s) at each ATP concentration is also estimated by graphical extrapolation of the slow phase back to time zero. Finally, the observed rate constant for the fast phase is deduced from the initial phase of the reaction, which is comprised of both the fast and slow reaction phases; the slow phase is subtracted from the data at early times in a pointwise fashion, and the subtracted data are replotted to reveal the graphically estimated fast phase rate constant, k_I^{obs}. The graphically-estimated and computer-fitted rate constants were generally in good agreement.

The observed rate constants were replotted in order to determine the intrinsic constants for the fast and slow phases (Figure 2A,B). These results show that both the fast and slow phases demonstrated saturable behavior. There was no evidence that would support a higher order reaction in terms of ATP concentration; i.e., terms such as $[ATP]^2$ are not required in eq 2–4. The data for the CKD indicated that the ATP concentration range used (50–400 μM) was sufficient for a good determination of parameters in both phases (Figure 2). Data for native insulin receptor in the absence of insulin indicated that the slow phase parameters were better determined. However, in the case of the native insulin receptor in the presence of 1 μM insulin, the ATP concentration range (5–100 μM [γ-^{32}P]ATP) appeared sufficient to nearly saturate the slow phase at all but the lowest concentration. Data collected for the fast phase fall somewhat short of completeness, but the concentration range employed was limited by high background radioactivity at high ATP concentrations and the necessarily limited quantities of native receptor used in these reactions. Therefore, kinetic parameters were derived by successive approximations of the experimentally determined data for the insulin-stimulated receptor. Similarly, the two parameters relating to the partition function, Φ_f and K_f (Figure 2C), were determined for the CKD alone and for the native insulin receptor in the absence or presence of insulin. This function shows saturation with increasing ATP concentrations,

[2] In deriving a Michaelis–Menten equation, the steady-state assumption of $d(ES)/dt = 0$ is in fact applied to all forms of the enzyme. This includes the free enzyme as well as the Michaelis complex per se.

Table I: Kinetic Parameters of Autophosphorylation[a]

constant	CKD	native receptor	
		-insulin	+insulin
k_I (min^{-1})	0.55 ± 0.07	0.20 ± 0.04	2.3 ± 0.3
k_{II} (min^{-1})	0.015 ± 0.004	0.008 ± 0.002	0.03 ± 0.01
K_I (μM)	130 ± 25	120 ± 20	180 ± 20
K_{II} (μM)	60 ± 12	50 ± 8	8 ± 2
K_F (μM)	≈180	≈40	≈15
Φ_f	0.3	0.48	0.83

[a] Kinetic parameters were determined by graphical and computer-based fitting of the experimental data from time courses of autophosphorylation (see Figures 1 and 2).

with the fraction proceeding by the fast phase increasing with increasing ATP concentration. As indicated by eq 4, the fraction in the slow phase decreases in concert with the increase in the fast phase.

The kinetic parameters thus obtained (Table I) demonstrate two important points: *First*, insulin stimulation of autophosphorylation results primarily from two factors. There is an approximately 10-fold increase of the intrinsic rate *constant*, k_I, for the fast phase of the reaction. There is also a transition in the maximum fraction of autophosphorylation that can proceed by this fast phase (see Φ_f in Table I). Taken together, under insulin stimulation there can be a net 20-fold increase in the fast phase *rate*, by a combination of the increased rate constant and a near-doubling of the fraction in the fast phase. There is no significant difference in the saturation of the fast phase, indicated by the comparable values for K_I. Furthermore, insulin does not appear to have as significant an impact on the intrinsic rate constant for the slow phase, k_{II}, although insulin seems to substantially raise the degree of saturation of this reaction at each ATP concentration, indicated by the lower value of K_{II}.

Second, autophosphorylation of the cytoplasmic kinase domain is kinetically more similar to autophosphorylation of the native insulin receptor, in the absence of insulin (Table I). There is a difference in the degree of saturation for the slow-to-fast phase transition, indicated by K_f. There is also a difference in the fast phase intrinsic rate constant, but it is substantially less than the difference due to insulin stimulation of the native receptor.

Dependence of Autophosphorylation Sites on ATP Concentration. There are seven specific tyrosyl groups in the insulin receptor that undergo autophosphorylation. These sites are clustered in three subdomains of the intracellular process of the insulin receptor's β-subunit, i.e., the cytoplasmic kinase domain. These subdomains, or regions, are the juxtamembrane region, the central region, and the carboxy-terminal region. After autophosphorylation with [γ-^{32}P]ATP, tryptic [^{32}P]phosphopeptides that contain each of these sites can be mapped by reverse-phase HPLC. The characteristic elution positions, amino acid sequences, and thus the subdomain identities are known (Kohanski, 1993, and references cited therein).

Given this information, we asked if certain autophosphorylation sites or regions reacted exclusively by one kinetic phase, or if these sites display a "preference" for one kinetic phase over the other. We examined the tryptic [^{32}P]phosphopeptide maps for the sites/subdomains that reacted during autophosphorylation for a fixed time at different concentrations of [γ-^{32}P]ATP (Figure 3). The major autophosphorylation sites undergoing reaction differ dramatically between the two ATP concentrations used in the basal state insulin receptor (Figure 3, panel A *versus* panel B) and also comparing the effect of

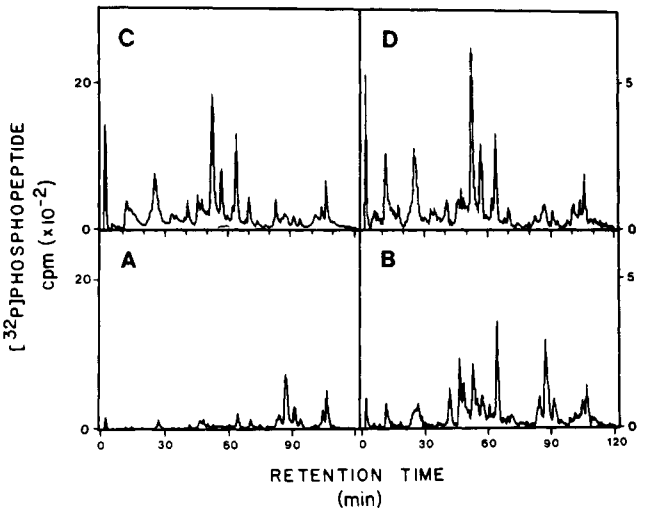

FIGURE 3: Representative tryptic [^{32}P]phosphopeptide maps. Native insulin receptor was autophosphorylated in the absence (panels A and B) or the presence (panels C and D) of 1 μM insulin for 30 min. The concentration of [γ-^{32}P]ATP was 10 μM (panels A and C) or 100 μM (panels B and D). The identities of each phosphopeptide are given in detail in the following paper (Kohanski, 1993). The domains from which these tryptic [^{32}P]phosphopeptides originated were as follows: central domain, 12–46 min; carboxy-terminal domain, 47–66 min; and juxtamembrane domain, 70–105 min.

insulin at each ATP concentration (Figure 3, panel A *versus* panel C, and panel B *versus* panel D).

Similar experiments were performed over a broader range of [γ-^{32}P]ATP concentrations for both the native insulin receptor and for the cytoplasmic kinase domain. For each reaction condition, tryptic phosphopeptide maps were generated and analyzed for the quantities of [^{32}P]phosphopeptides derived from each subdomain (Figure 4). Low ATP concentrations favored reaction in the juxtamembrane region of the CKD (Figure 4A) and also in the basal state insulin receptor (Figure 4B). With increasing ATP concentrations, the relative percent of reaction in the juxtamembrane region decreased while the relative extents of reaction in the central and carboxy-terminal regions increased. At each ATP concentration examined, the percentage distributions among these subdomains were similar, comparing the CKD with the basal state insulin receptor (Figure 4, panel A *versus* panel B).

A similar effect of increasing ATP concentrations was observed with insulin-stimulated native receptor (Figure 4C). However, while the percentage contribution of the juxtamembrane subdomain decreased and the contribution of the carboxy-terminal subdomain increased, the central domain generally contributed a constant 25% of the net reaction (25.7 ± 2.1%) over the entire concentration range in Figure 4C. Comparing the insulin-stimulated with the basal state receptor at each ATP concentration, the percentage of net reaction in the juxtamembrane region was always lower in the stimulated state (Figure 4, panel B *versus* panel C).

These data were further analyzed for the fold-stimulation by insulin of net autophosphorylation *and* the stimulation within each subdomain (Table II). The observed fold-stimulation of net autophosphorylation at this time point decreased with increasing ATP concentration. The calculated fold-stimulation of net autophosphorylation by insulin, based on the kinetic constants, was in good agreement with the observed values. In terms of the subdomains, the least stimulation occurred in the juxtamembrane subdomain at all ATP concentrations. The observed fold-stimulations within the central and carboxy-terminal domains were generally close

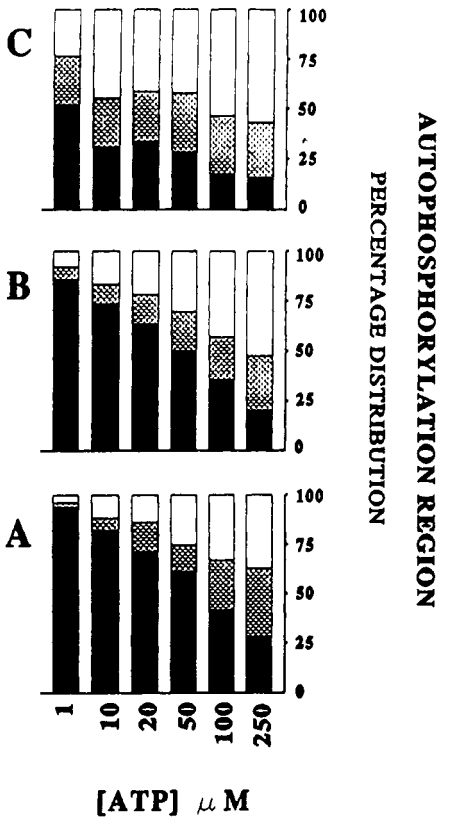

FIGURE 4: Percentage distribution of autophosphorylation among the three autophosphorylation regions. Primary data were taken from tryptic [^{32}P]phosphopeptide maps (cf. Figure 3). The quantity of ^{32}P found in each autophosphorylation region, after a 30-min reaction at the indicated concentration of [γ-^{32}P]ATP, was determined, and these were replotted as the percentage of the total ^{32}P in all three regions as (from bottom to top) juxtamembrane region (solid bars), central region (cross-hatched bars), and carboxy-terminal region (open bars). These results are shown for autophosphorylation of (panel A) 0.25 μM CKD, (panel B) $\approx$ 5 nM native insulin receptor alone, and (panel C) native insulin receptor in the presence of 1 μM insulin.

to each other, and these values also decreased with increasing ATP concentration. These results show that the major stimulatory effects of insulin are in the central and carboxy-terminal autophosphorylation regions.

DISCUSSION

The autophosphorylation reaction was analyzed by an equation that used the sum of two exponentials. Michaelis–Menten kinetics were considered inappropriate because the autophosphorylation reaction does not fit two essential preconditions of initial velocity kinetics: *First*, pseudo-first-order conditions cannot be met for the phosphate-acceptor substrate because the enzyme is itself the substrate. Therefore, the phosphate-acceptor substrate cannot be made in excess over the enzyme concentration. However, pseudo-first-order conditions can be met for ATP concentration, and indeed these are necessary in this analysis as for Michaelis–Menten kinetics. *Second*, enzyme turnover in this reaction is unique because it is intramolecular; the enzyme is also the product. Although there are individual catalytic events—phosphoryl transfers—the apoenzyme at the beginning of each event is not the same as the phosphoenzyme after the event. Thus the steady-state condition *per se* does not apply to "free" enzyme, as it must in classical initial velocity experiments.[2] The observation of two kinetic phases (see Figure 1) means that there are two discrete reaction rates in the early part of the reaction, and this would lead to nonhyperbolic saturation

Table II: Fold-Stimulation by Insulin of the Native Receptor[a]

[ATP] (μM)	fold-stimulation[b] net[c] obs	(calc)	subdomain juxtamembrane	central	carboxy-terminal
10	5.6	(8.3)	1.8	19.8	21.4
20	3.0	(4.9)	1.6	5.1	5.8
50	2.1	(2.7)	1.4	3.0	2.8
100	1.9	(2.1)	1.0	2.6	2.4
250	1.3	(1.8)	1.1	1.3	1.5

[a] The fold-stimulation by insulin of the net reaction and of autophosphorylation in each of the three subdomains was analyzed for reactions performed at the indicated concentrations of [γ-^{32}P]ATP. Data were from reverse-phase HPLC maps of tryptic [^{32}P]phosphopeptides, as illustrated in Figure 3. [b] A value of 1 means no stimulation was observed. [c] The observed (obs) net stimulation was taken from each reaction used to generate data shown in Figure 4, except data for the reaction at 1 μM ATP, since the percentages in the latter two domains were too low for a reliable determination of the fold-stimulation. The calculated (calc) net stimulation was predicted using eq 1 and the kinetic parameters given in Table I.

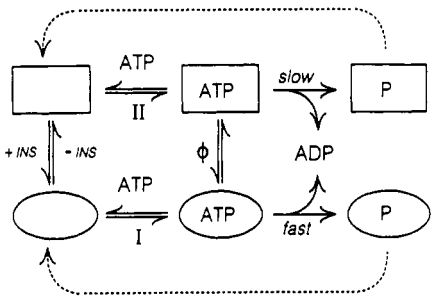

FIGURE 5: Kinetic model for autophosphorylation. This scheme for autophosphorylation shows two states of the kinase, disposed to react in the slow phase (rectangle, and the upper pathway indicated II) or in the fast phase (ellipse, and the lower pathway indicated I). The apoenzyme is shown by open symbols and the phosphoenzyme by a "P" within the symbol. A reversible complex is formed between the enzyme and ATP, which may be followed by an isomerization (the step indicated as ϕ). In the absence of insulin, most of the enzyme will be in the slow phase conformer and would partition more toward the fast phase conformer with increasing ATP concentrations. In the presence of insulin, population of the fast phase conformer would be greater. Because insulin is an allosteric regulator of the receptor, its effect on conformer distribution is shown separately. Autophosphorylation occurring after the first catalytic event is shown by the dashed lines. Interconversion of the fast and slow phase *phospho*-enzyme conformers is not shown for reasons stated in the text.

behavior if one measured only the initial rates of reaction.

Kinetic Model. We therefore adapted a kinetic scheme employed by Hess and co-workers for bungarotoxin binding to the acetylcholine receptor (Bulger et al., 1977). This scheme treats the forward reaction as the sum of two exponentials or kinetic phases (eq 1), such that most kinetic parameters can be extracted from graphical analyses (Figures 1 and 2). Both the fast and slow kinetic phases of the reaction were saturable with ATP (Figire 2A,B). Partition of the reaction between fast and slow phases was also saturable with ATP (Figure 2C).

These features of the reaction, even for a monomeric enzyme, have led us to propose a reaction scheme for intramolecular autophosphorylation (Figure 5). Two interconvertible forms of the kinase are indicated by the rectangle (higher affinity for ATP, slow reaction phase) and the ellipse (lower affinity for ATP, fast reaction phase). Insulin and ATP are shown favoring the fast reaction phase, as required by our observations. Considering the reaction for the first phosphorylation event in the basal state, the enzyme is predominantly in the slow phase conformer. Upon ATP binding, the slow phase conformer would equilibrate with the fast phase conformer,

but in the basal state and at low ATP concentrations, the slow phase conformer is still favored and the reaction is dominated by the slow phase kinetic parameters. Increasing ATP concentrations would determine the distribution between slow and fast conformers, governed by the partition function (shown as ϕ), such that raising the ATP concentration increases the fraction in the fast phase conformer. The insulin-stimulated state favors the fast phase conformer, even before the addition of ATP, and while insulin remains bound, the equilibration between enzyme–ATP complexes continues to favor the fast phase conformer, and the reaction is thus dominated by the fast phase kinetic parameters. We do not show equilibration between the two autophosphorylated states based upon the following: (1) The observation that autophosphorylation in the presence of insulin apparently fixes the insulin-stimulated state (Rosen et al., 1983; Yu et al., 1985; Yu & Czech, 1986); (2) autophosphorylation in the central subdomain is associated with activation (Ellis et al., 1986; Flores Riveros et al., 1989; Herrera & Rosen, 1986; Murakami & Rosen, 1991; Tornqvist & Avruch, 1988; White et al., 1988; Zhang et al., 1991); and (3) autophosphorylation in the central subdomain is primarily through the fast phase (this study).

The above discussion relates to the first catalytic event; i.e., phosphorylation of the first residue. The second autophosphorylation event would demonstrate partial hysteresis if it does not follow the same kinetic path as the first event; that is, kinase molecules that have initially autophosphorylated in the fast phase (via the central domain) would be fixed in the fast phase for subsequent autophosphorylation events, but those in the slow phase could be shifted into the fast phase by insulin and/or ATP. However, it is also possible that autophosphorylation within the carboxy-terminal subdomain does not fix the kinase in the fast phase conformer, since there is no evidence to implicate this subdomain in activation[3] of the enzyme. Therefore there are two potential contributors to partial hysteresis due to autophosphorylation in the juxtamembrane and/or carboxy-terminal subdomains.[4] This hysteresis would fit the observation that the lower affinity fast phase reaction increases with increasing ATP concentration, rather than an increase in the higher affinity slow phase of the reaction. This outline of the autophosphorylation reaction mechanism is consistent with the kinetic studies presented here.

Autophosphorylation Domains Correlate with Kinetic Phases. We could demonstrate that autophosphorylation subdomains are associated with the kinetic phases. The juxtamembrane sites are favored in the slow phase, and the fast phase favors the central and carboxy-terminal sites. These conclusions were reached after using the kinetic parameters (Table I) to calculate the percentage contribution of each kinetic phase to net autophosphorylation and then to compare these predictions to the observed distribution within each domain (Figure 4). For example, raising the ATP concentration decreases the slow kinetic phase contribution because the parameter ϕ_s is decreasing. For a 30-min reaction of the basal state insulin receptor, the percentage contribution by the slow phase is calculated to decrease as follows: 89% at 1 μM ATP, 50% at 10 μM ATP, and 23% at 100 μM ATP. We observed that the proportion of juxtamembrane sites decreased with increasing ATP concentration: 85%, 68%, and 37% at the same respective ATP concentrations (Figure 4B). This correlation suggests that reaction of the juxtamembrane sites is associated with the slow kinetic phase, especially for the autophosphorylation reaction in the absence of insulin. In the insulin stimulated state, the percentage contribution of the slow phase to net autophosphorylation is calculated to be 82%, 45%, and 18% at 1, 10, and 100 μM ATP, respectively, and the observed values for the juxtamembrane sites were 52%, 28%, and 17%, respectively (Figure 4C). Thus the slow phase contribution declines with increasing ATP concentration, and these are matched fairly well by the decline in the contribution of the juxtamembrane sites. Also, the contribution of both the slow phase and the juxtamembrane sites are lower in the presence of insulin (Figure 4, panel C *versus* panel B), consistent with the decreasing fold-stimulation within the juxtamembrane domain (Table II). Because the distribution between fast and slow kinetic phases is complementary, we conclude that the central and carboxy-terminal subdomains' sites react preferentially in the fast kinetic phase. In addition, the latter two autophosphorylation subdomains showed parallel changes and similar values in their fold-stimulation by insulin (Table II); they apparently both react in the same (fast) kinetic phase.

Cis- versus Trans-Subunit Autophosphorylation. Cobb *et al.* (1989) showed that CKD autophosphorylation was concentration dependent and concluded that the reaction occurred between monomers or by a "transphosphorylation" mechanism. Data to support the contrary view were presented by Villalba *et al.* (1989), showing that CKD autophosphorylation was intramolecular or by "cisphosphorylation". Studies on several forms of the heterotetrameric receptor by Treadway *et al.* (1991) demonstrated exclusively transphorylation of the reconstituted "native" receptor, whereas recent data from Lee *et al.* (1993) are consistent with both cis- and transphosphorylation within/between β-subunits of the native receptor.

Against this background, our kinetic analysis of CKD autophosphorylation was based on an *intra*molecular reaction. In preliminary experiments, we found no concentration dependence for CKD autophosphorylation, in agreement with Villalba *et al.*, (1989), which justifies our approach. However, Cobb *et al.* (1989) used polycationic activators of autophosphorylation, which promote aggregation (cf. Kohanski, 1990) and perhaps induce transphosphorylation between monomers. Our results therefore demonstrate that all autophosphorylation sites are *accessible* by intramolecular reactions; this does not exclude trans-subunit phosphorylation in the native receptor. The kinetic model addresses only intra*molecular* autophosphorylation and does not resolve the issue of whether or not there is transphosphorylation between subunits in the intact receptor. The activating effect of insulin on native receptor autophosphorylation is reflected by changes in two kinetic parameters of the fast phase, the rate constant, k_1, and the initial disposition of sites to react by the fast phase, Φ_f (Table I). If insulin promotes trans-subunit phosphorylation, then the fast-phase sites would be favored in the trans-reaction because they are favored in the fast phase, and these are the

[3] Activated state refers to the increased rate of substrate phosphorylation due to insulin stimulated autophosphorylation (Rosen et al., 1983; Yu & Czech, 1986; Yu et al., 1985; Kohanski & Lane, 1986).

[4] This model is consistent with the conclusion that the sites of autophosphorylation react in a "random" order (Tonqvist & Avruch, 1988) rather than in a specific order beginning with the central domain (White et al., 1988). The data presented in Figure 3A, showing substantial reaction in the juxtamembrane subdomain, without significant reaction in the central subdomain also favor the "random-order" site-wise autophosphorylation model and do not support the conclusion of reaction in the central subdomain as the obligatory first locus of autophosphorylation. It is not clear that the order of reaction is *completely* random, but we have no additional evidence that would permit firmer conclusions on this point.

[5] There are differing opinions on whether or not a single mechanism of stimulation is common to polycations and insulin (Biener & Zick, 1990, 1991; Fujita-Yamaguchi et al., 1989a,b; Morrison et al., 1989).

sites showing the greatest stimulation by insulin. Thus the parameter Φ_f may be correlated with increased trans-subunit autophosphorylation or with allosteric interactions between subunits. Either or both of these possibilities might correlate with known insulin-dependent conformational changes in the native receptor (Schenker & Kohanski, 1988; Waugh & Pilch, 1989).

Comparing the CKD with the Native Receptor. A final result of this study is the comparison of the cytoplasmic kinase domain with the native insulin receptor. It has been reported by others that autophosphorylation of the CKD mimics autophosphorylation of the insulin stimulated receptor (Cobb et al., 1989; Tavare et al., 1991). We do not find this to be the case. Kinetically, the CKD behaves in a manner more like the basal state insulin receptor than the insulin stimulated receptor (Table I). Whatever weight is given to the kinetic analysis, our observations of the subdomain distributions (Figure 4, panel A *versus* panel B) conclusively demonstrated similar patterns of autophosphorylation at each ATP concentration tested. Where other groups have concluded that the CKD is a model for the insulin-stimulated receptor, in fact those experiments used a stimulatory agent for the autophosphorylation reactions involving the CKD (Cobb et al., 1989; Tavare et al., 1991). Indeed, other stimulatory agents such as polycations can mimic the insulin stimulated phosphopeptide map (Kohanski, 1989) while employing an apparently different mechanism for stimulation.[5] We have shown previously that CKD autophosphorylation was subject to peptide stimulation in a manner similar to the basal state native receptor (Kohanski & Schenker, 1991), whereas insulin-activated native receptor autophosphorylation was inhibited by these same peptides. As will be discussed in the following paper, the [^{32}P]phosphopeptide maps used in that analysis suffered from certain artifacts, but the qualitative conclusion remains unaltered: the CKD is a model for basal state autophosphorylation, and the *stimulated* CKD is a good model for the *stimulated* receptor in terms of the resulting autophosphorylation sites. It is hoped that the results presented in this study will enhance the applicability of the cytoplasmic kinase domain as a model for both the unstimulated and insulin-stimulated insulin receptor.

In summary, we have shown that juxtamembrane autophosphorylation sites react more slowly than central or carboxy-terminal domain sites, that the slower reacting sites are favored at low ATP concentrations, and that insulin favors reaction in at the fast-reacting sites, and we have presented a novel kinetic model consistent with these findings.

ACKNOWLEDGMENT

The author thanks Dr. Paul F. Pilch for making his manuscript (Lee *et al.*, 1993) available in advance of publication.

REFERENCES

Backer, J. M., Schroeder, G. G., Cahill, D. A., Ullrich, A., Siddle, K., & White, M. F. (1991) *Biochemistry 30*, 6366.
Biener, Y., & Zick, Y. (1990) *Eur. J. Biochem. 194*, 243.
Biener, Y., & Zick, Y. (1991) *J. Biol. Chem. 266*, 17369.
Bulger, J. E., Fu, J.-L., Hindy, E. F., Silberstein, R. L., & Hess, G. P. (1977) *Biochemistry 16*, 684.
Carlson, G. M., & Graves, D. J. (1976) *J. Biol. Chem. 251*, 7480.
Cobb, M. H., Sang, B. C., Gonzalez, R., Goldsmith, E., & Ellis, L. (1989) *J. Biol. Chem. 264*, 18701.
Ellis, L., Clauser, E., Morgan, D. O., Edery, M., Roth, R. A., & Rutter, W. J. (1986) *Cell 45*, 721.
Ellis, L., Tavare, J. M., & Levine, B. A. (1991) *Biochem. Soc. Trans. 19*, 426.
Flores Riveros, J. R., Sibley, E., Kastelic, T., & Lane, M. D. (1989) *J. Biol. Chem. 264*, 21557.
Fujita-Yamaguchi, Y., Kathuria, S., Xu, Q. Y., McDonald, J. M., Nakano, H., & Kamata, T. (1989a) *Proc. Natl. Acad. Sci. U.S.A. 86*, 7306.
Fujita-Yamaguchi, Y., Sacks, D. B., McDonald, J. M., Sahal, D., & Kathuria, S. (1989b) *Biochem. J. 263*, 813.
Hallenbeck, P. C., & Walsh, D. A. (1983) *J. Biol. Chem. 258*, 13493.
Herrera, R., & Rosen, O. M. (1986) *J. Biol. Chem. 261*, 11980.
Huang, K.-P., Chan, K.-F. J., Singh, T. J., Nakabayashi, H., & Huang, F. L. (1986) *J. Biol. Chem. 261*, 12134.
Kohanski, R. A. (1989) *J. Biol. Chem. 264*, 20984.
Kohanski, R. A. (1993) *Biochemistry* (following paper in this issue).
Kohanski, R. A., & Lane, M. D. (1983) *J. Biol. Chem. 258*, 7460.
Kohanski, R. A., & Lane, M. D. (1985) *J. Biol. Chem. 260*, 5014.
Kohanski, R. A., & Lane, M. D. (1986) *Biochem. Biophys. Res. Commun. 134*, 1312.
Kohanski, R. A., & Schenker, E. (1991) *Biochemistry 30*, 2406.
Laemmli, U. K. (1970) *Nature 227*, 680.
Lai, Y., Nairn, A. C., & Greengard, P. (1986) *Proc. Natl. Acad. Sci. U.S.A. 83*, 4253.
Lee, J., O'Hare, T., Pilch, P. F., & Shoelson, S. E. (1993) *J. Biol. Chem. 268*, 4092.
Morrison, B. D., Feltz, S. M., & Pessin, J. E. (1989) *J. Biol. Chem. 264*, 9994.
Murakami, M. S., & Rosen, O. M. (1991) *J. Biol. Chem. 266*, 22653.
O'Hare, T., & Pilch, P. F. (1988) *Biochemistry 27*, 5693.
Olefsky, J. M. (1990) *Diabetes 39*, 1009.
Palmer, J. L., & Avruch, J. (1981) *Anal. Biochem. 116*, 372.
Reidel, H., Dull, T. J., Honegger, A. M., Schlessinger, J., & Ullrich. A. (1989) *EMBO J. 8*, 2943.
Rosen, O. M., & Erlichman, J. (1975) *J. Biol. Chem. 250*, 7788.
Rosen, O. M., Herrera, R., Olowe, Y., Petruzzelli, L. M., & Cobb, M. H. (1983) *Proc. Natl. Acad. Sci. U.S.A. 80*, 3237.
Schenker, E., & Kohanski, R. A. (1988) *Biochem. Biophys. Res. Commun. 157*, 140.
Tavare, J. M., Clack, B., & Ellis, L. (1991) *J. Biol. Chem. 266*, 1390.
Tornqvist, H. E., & Avruch, J. (1988) *J. Biol. Chem. 263*, 4593.
Treadway, J. L., Morrison, B. D., Soos, M. A., Siddle, K., Olefsky, J., Ullrich, A., McClain, D. A., & Pessin, J. E. (1991) *Proc. Natl. Acad. Sci. U.S.A. 88*, 214.
Ullrich, A., & Schlessinger, J. (1990) *Cell 64*, 203.
Villalba, M., Wente, S. R., Russell, D. S., Ahn, J. C., Reichelderfer, C. F., & Rosen, O. M. (1989) *Proc. Natl. Acad. Sci. U.S.A. 86*, 7848.
Walseth, T. F., & Johnson, R. A. (1979) *Biochim. Biophys. Acta 562*, 11.
Waugh, S. M., & Pilch, P. F. (1989) *Biochemistry 28*, 2722.
White, M. F., Haring, H.-U., Kasuga, M., & Kahn, C. R. (1984) *J. Biol. Chem. 259*, 255.
White, M. F., Shoelson, S. E., Keutmann, H., & Kahn, C. R. (1988) *J. Biol. Chem. 263*, 2969.
Whittaker, J., Okamoto, A. K., Thys, R., Bell, G. I., Steiner, D. F., & Hofmann, C. A. (1987) *Proc. Natl. Acad. Sci. U.S.A. 84*, 5237.
Yu, K. T., & Czech, M. P. (1986) *J. Biol. Chem. 261*, 4715.
Yu, K. T., Pessin, J. E., & Czech, M. P. (1985) *Biochimie 67*, 1081.
Zhang, B., Tavare, J. M., Ellis, L., & Roth, R. A. (1991) *J. Biol. Chem. 266*, 990.